Synchronization of stochastic mean field networks of Hodgkin-Huxley neurons with noisy channels

Mireille Bossy, Joaquin Fontbona, Héctor Olivero Quinteros

Synchronization of stochastic mean field networks of Hodgkin-Huxley neurons with noisy channels.

Mireille Bossy[*] Joaquín Fontbona[†] and Héctor Olivero[‡]

January 18, 2018

Abstract

In this work we are interested in a mathematical model for collective behavior of a fully connected network of finitely many neurons when their number and when time go to infinity. We assume that every neuron follows a stochastic version of the Hodgkin-Huxley model, and that pairs of neurons interact through both electrical and chemical synapses, the global connectivity being of mean field type. When the leak conductance is strictly positive, we prove that if the initial voltages are uniformly bounded and the electrical interaction between neurons is strong enough, then, uniformly in the number of neurons, the whole system synchronizes exponentially fast as time goes to infinity, up to some error controlled by (and vanishing with) the channels noise level. Moreover, for exchangeable random initial conditions and arbitrary interaction intensity, we prove that on every bounded time interval the propagation of chaos property for this system holds. Combining these results, we deduce that the nonlinear McKean-Vlasov equation describing an infinite network of such neurons concentrates, as times goes to infinity, around the dynamics of a single Hodgkin-Huxley neuron with a chemical neurotransmitter channel. Our results are illustrated and complemented with numerical simulations.

1 Introduction

The dynamics of a neuron's voltage is the result of the passage of ions through its membrane. This ion flux takes place through specific proteins which act as gated channels. According to the Hodgkin-Huxley model of a nerve neuron [26], the coupled behavior of the voltage of the neuron V_t, with the proportions m_t, h_t and n_t of open channels of the different ions involved in this process (respectively activation Sodium channels, deactivation Sodium channels and activation Potassium channels), can be described by the following system of ordinary differential equations:

$$\begin{aligned} V_t &= V_0 + \int_0^t F(V_s, m_s, n_s, h_s) ds \\ x_t &= x_0 + \int_0^t \rho_x(V_s)(1 - x_s) - \zeta_x(V_s) x_s \, ds \end{aligned} \tag{1.1}$$

where, here and in the sequel, x generically represents the m, n, h components and $F : \mathbb{R} \times [0,1]^4 \to \mathbb{R}$, defined by

$$F(V, m, n, h) = I - g_{\mathrm{K}} n^4 (V - V_{\mathrm{K}}) - g_{\mathrm{Na}} m^3 h (V - V_{\mathrm{Na}}) - g_{\mathrm{L}} (V - V_{\mathrm{L}}), \tag{1.2}$$

[*]INRIA Sophia Antipolis Méditerranée, France, Mireille.Bossy@inria.fr

[†]Center for Mathematical Modeling, University of Chile. fontbona@dim.uchile.cl. Supported by CMM-Basal Conicyt, Nucleo Milenio NC 130062 and Fondecyt Grant 1150570

[‡]INRIA Sophia Antipolis Méditerranée, France. CIMFAV, Facultad de Ingeniería, Universidad de Valparaíso. General Cruz 222, Valparaíso, Chile. hector.olivero-quinteros@inria.fr. Partially supported by Nucleo Milenio NC 130062 and by Beca Chile Postdoctorado.

This research was partially supported by the supercomputing infrastructure of NLHPC (ECM-02), Conicyt.

represents the effect on the voltage of the ionic channels and of an external current I (assumed constant for simplicity). The rate functions ρ_x and ζ_x, originally considered in [26], have some generic form given in (2.3) and (2.4) below; see also Figure 1 and Tables 2 and 1 for their shape and for biologically meaningful values of the parameters. We refer the reader to Ermentrout and Terman [14] for a concise discussion on the Hodgkin-Huxley (HH in the sequel) model and its deduction, as well as for general background on mathematical neuroscience models.

From a mathematical point of view, system (1.1) defines a rich dynamical system, the properties of which has been extensively studied. As an example of its various possible behaviors, Figure 2 below illustrates different possible responses of system (1.1) to the value of the input current I, all other parameters of the model being fixed. See e.g. [14] and Izhikevich [28], and references therein for detailed accounts on dynamical properties of (1.1) and related neuron models. Lower dimensional dynamics have also been proposed as simpler alternatives to (1.1), the most important ones being the FitzHugh-Nagumo model (FitzHugh [16], Nagumo et al. [37]) and the Morris-Lecar model (Morris and Lecar [36]). These are able to reproduce some of the dynamical features of the HH system (1.1) and are easier to study from the mathematical point of view, but they are less realistic regarding some of its relevant features.

A different approach to model the electric activity of neurons are integrate-and-fire models, introduced in Lapicque [32]. In these models the electric potential evolves according to some ordinary differential equation until it reaches a certain fixed threshold; the neuron then emits a potential spike and the voltage is reset to some reference value, from which its evolution restarts following the same dynamics. We refer the reader to Burkitt [9] and Burkitt [10] for a review of this class of models.

In the last decade, there has been an increasing interest of the mathematical and computational neuroscience communities in understanding the role of stochasticity in neurons' dynamics, as well as in mathematical models for it. We refer the reader to Goldwyn et al. [22] and to Goldwyn and Shea-Brown [23] for a discussion on different ways in which randomness might be introduced in the HH model, their biological interpretation and their pertinence. See also [14, Chapter 10] for general background on this issue. Classically, random models arise in the form of finite Markov chains describing a discrete number of open gates which approximate the ion channel dynamics, or by directly introducing Gaussian additive or multiplicative white noise (that is, a Brownian motion or a stochastic integral with respect to it) in the voltage or ion channels dynamics in (1.1). More recently, hybrid (also called piecewise deterministic) Markov processes have also been proposed as microscopic counterparts of the HH or other deterministic models. In this setting, the channel variables are replaced by discrete continuous time processes whose jump rates depend on the voltage, while keeping a continuous description for the latter, see Austin [2], Pakdaman et al. [39] and references therein. We also refer the reader to Bossy et al. [8], Dangerfield et al. [12], Wainrib [44] and Sacerdote and Giraudo [41] for further discussion on stochastic models in this context, the latter one in the case of integrate-and-fire models.

In the present work we consider stochastic versions of the HH model (1.1) which arise as diffusive scaling limits of hybrid models of the type studied in [2] and [39]. More precisely, we are interested in networks of N such neurons in mean field interaction, which can be described by a system of stochastic differential equations of the form:

$$\begin{aligned} V_t^{(i)} &= V_0^{(i)} + \int_0^t F(V_s^{(i)}, m_s^{(i)}, n_s^{(i)}, h_s^{(i)})ds \\ &\quad - \int_0^t \frac{1}{N}\sum_{j=1}^N J_{\mathrm{E}}(V_s^{(i)} - V_s^{(j)}) - \frac{1}{N}\sum_{j=1}^N J_{\mathrm{Ch}} y_s^{(j)}(V_s^{(i)} - V_{\mathrm{rev}})ds, \\ x_t^{(i)} &= x_0^{(i)} + \int_0^t b_x(V_s^{(i)}, x_s^{(i)})ds + \int_0^t \sigma_x(V_s^{(i)}, x_s^{(i)})dW_s^{x,i}, \quad x = m, n, h, y. \end{aligned}$$

Here, $(W^{x,i} : i = 1, \dots, N, x = m, n, h, y)$ are one dimensional Brownian motions and the interaction between neurons account for the effect of electrical and chemical synapses (the biological interpretation of the interactions terms and in particular of the variables $y^{(i)}$ is given in next section). We refer to equation (2.1) below for the explicit form of the system we will consider, and for Hypothesis 2.1 for our assumptions on its coefficients.

The collective behavior of neurons, and the way it emerges from their individual features and synaptic activity, is inndeed a central question in neuroscience. In particular, considerable efforts have been devoted to understanding synchronization of neurons, an ubiquitous phenomenon seemingly related to the generation of rhythms (such as the respiratory one or the heartbeat) but also to

more complex neurologic functionalities. For instance, at the brain level, synchronization has been connected to memory formation, see Axmacher et al. [3], but also to disorders such as epileptic seizures, see Jiruska et al. [29]. Since the neuroscience literature on this topic is huge, it is not our intention to thoroughly comment on it here, and we refer the reader to [14, Chapters 8,9], [28, Chapter 10] for further discussion on biological roles of neuron synchronization, and mathematical approaches to it. A central mathematical tool in this setting, introduced by Kuramoto [31], is phase reduction, which is based on the idea that stable periodic solutions of a nonlinear oscillator can be parametrized by its phase in the limit cycle. Kuramoto's model has proved useful to understand synchronization mechanisms of simple coupled oscillators (see [14] and [28]), even in the limiting case of infinite oscillators with noise and mean field interaction (see Bertini et al. [5] and the discussion in [44, Chapter 4]). However, to our knowledge, applications of these ideas to networks of HH-type neurons have so far been restricted to small deterministic networks and "weak coupling" regimes (see e.g. Hansel and Mato [24] and Hansel et al. [25]). We refer the reader to Ostojic et al. [38] for synchronization results in the case of integrate-and-fire networks.

A related question is the asymptotic behavior of networks when the number of neurons tends to infinity. In that sense, networks of N neurons in mean field interaction, in which every neuron experiences a pairwise interaction of strength-order $1/N$ with each other, provide a mathematically tractable (though not completely realistic) framework to address this question. Indeed, in a mean field network, the evolutions of finitely many neurons are expected to become independent as N goes to infinity, a property known as propagation of chaos. In the case of exchangeable particles, this is equivalent to the convergence of the dynamics of the empirical law of the system to some deterministic flow of probability laws, typically described by a nonlinear McKean-Vlasov partial differential equation (also termed "mean field" equation in this context); see Méléard [34], Sznitman [42] for background on propagation of chaos. We refer the reader to e.g. Faugeras et al. [15] for formal derivations of mean field equations for multi type population networks of integrate-and-fire neurons, and respectively to Delarue et al. [13] and Perthame and Salort [40] for probabilistic and PDE approaches to the global solvability of that equation (which can in principle have explosive solutions) when the interaction is small. See also Fournier and Löcherbach [17] for further recent results on propagation of chaos for integrate and fire models. The propagation of chaos for mean field networks of neurons described by stochastic differential equations, including stochastic, multi type HH and FitzHugh-Nagumo networks, has been addressed in Baladron et al. [4], and then rigorously established in Bossy et al. [8]. We also refer the reader to Mischler et al. [35] for the mean field description of a network of FitzHugh-Nagumo neurons.

In this present work, we establish that, under strong enough electrical connectivity of the network (i.e. large enough J_E), the N neurons get synchronized, up to an error proportional to the channels' noise level σ^2, at an exponential rate which is independent of N. Moreover, we exhibit a deterministic single-neuron dynamics which is "mimicked", as time goes to infinity, by every neuron of the system (2.1), over short enough moving time-windows, up to an error that vanishes with σ^2 and N^{-1}. As far as we know, this is a first mathematical result which establishes the synchronization of large networks of neurons. We also establish the propagation of chaos for system (2.1), or its convergence to solutions to a McKean-Valsov equation, for arbitrary parameters of the model (and for slightly more general coefficients than in [8] in the single population case). This allows us to transfer our synchronization results to the limiting PDE, which can be understood as the description of an infinite network of neurons. Moreover, we establish the uniqueness of solutions to this equation (under slight regularity assumptions). Our theoretical results will be complemented with simulations, which in particular point out that synchronization phenomena might also hold for small electrical connectivity and even for pure chemical connectivity ($J_{\mathrm{E}} = 0$).

The remainder of the paper is organized as follows. In Section 2, we detail the model we consider and state precisely our main results. Section 3 is devoted to numerical experiments, both as illustration and further analysis of our theoretical statement. We also discuss therein possible improvements and extensions of our results, and some open questions. The mathematical proofs of our results are given in the Appendix sections.

2 Model and main results

We start by briefly recalling how chemical and electrical synapses in networks of neurons are modeled (we follow [14, Chapter 7] which we also refer to for further background on synaptic channels).

In chemical synapses, a neurotransmitter is released to the intercellular media (technically the synaptic cleft), from a pre-synaptic neuron to the post-synaptic one through synaptic channels, which are voltage-gated just as ion channels are. With each pre-synaptic neuron we can thus associate a new variable y in $[0,1]$ which represents its proportion of open synaptic channels at each time. The dynamics of this variable can be modeled in a similar way as those of ion channels, that is, in terms of certain rate functions ρ_y and ζ_y depending on the membrane potential V of that same neuron, and on some parameters (see (2.5)). The choice of these parameters determines the characteristic (inhibitory or excitatory) of the chemical synapse. Hence, in a fully connected network of N similar neurons, chemical synapses coming from a pre-synaptic neuron j should induce on the voltage $V^{(i)}$ of the post-synaptic neuron i an instantaneous variation at time t of

$$-\frac{J_{\text{Ch}}}{N} y_t^{(j)} (V_t^{(i)} - V_{\text{rev}}),$$

where $y_t^{(j)}$ is the proportion of open synaptic channels of neuron j, $J_{\text{Ch}} \geq 0$ is a constant representing the chemical conductance of the network and V_{rev} is a reference potential. The factor $\frac{1}{N}$ is introduced in order that the contribution of each incoming synapse to the neuron i has similar weight, which corresponds to a global interaction of mean field type.

On the other hand, the interior of one neuron can be directly connected with another neuron's one through an intercellular channel called gap junction, which allows the constant flow of ions between them, as a result of their possibly different potentials. We thus may assume that pre-synaptic neuron j contributes to the variation of the voltage of post-synaptic neuron i by the amount

$$-\frac{J_{\text{E}}}{N} (V_s^{(i)} - V_s^{(j)}),$$

where $J_{\text{E}} \geq 0$ is the electrical conductance (that can be thought of as a measure of the connectivity of the network) and the factor $\frac{1}{N}$ appears by similar reasons as before. Connections of this type are termed electrical synapses and are less frequent than chemical ones; on the other hand, they transmit information faster. (See also Hormuzdi et al. [27] for a deeper discussion on electrical synapses.)

In all the sequel, for each fixed N we consider a stochastic process $X = (X^{(1)}, \dots, X^{(N)})$ valued in $(\mathbb{R}^5)^N$, with coordinates $X_t^{(i)} = (V_t^{(i)}, m_t^{(i)}, n_t^{(i)}, h_t^{(i)}, y_t^{(i)})$ given for $i = 1, \dots, N$ and $t \geq 0$ by the solution of the system of stochastic differential equations:

$$\begin{aligned} V_t^{(i)} &= V_0^{(i)} + \int_0^t F(V_s^{(i)}, m_s^{(i)}, n_s^{(i)}, h_s^{(i)}) ds \\ &\quad - \int_0^t \frac{1}{N} \sum_{j=1}^N J_{\text{E}} (V_s^{(i)} - V_s^{(j)}) - \frac{1}{N} \sum_{j=1}^N J_{\text{Ch}} y_s^{(j)} (V_s^{(i)} - V_{\text{rev}}) ds, \\ x_t^{(i)} &= x_0^{(i)} + \int_0^t \rho_x(V_s^{(i)})(1 - x_s^{(i)}) - \zeta_x(V_s^{(i)}) x_s^{(i)} ds + \int_0^t \sigma_x(V_s^{(i)}, x_s^{(i)}) dW_s^{x,i}, \end{aligned} \tag{2.1}$$

where $(W^{x,i} : i \in \mathbb{N}, x = m, n, h, y)$ are independent one dimensional Brownian motions independent of X_0 and F is defined in (1.2). Notice that, for notational simplicity, the dependence of system (2.1) on N is omitted. Throughout this work, we will additionally make the following assumptions on system (2.1):

Hypothesis 2.1. *1. For $x = m, n, h$ and y, ρ_x and ζ_x are strictly positive, locally Lipschitz continuous functions defined on $\mathbb{R}$.*

2. For $x = m, n, h$ and y, functions $\sigma_x : \mathbb{R}^2 \to \mathbb{R}$ are given by

$$\sigma_x(v, z) = \sigma \sqrt{|\rho_x(v)(1 - z) + \zeta_x(v) z|} \chi(z), \tag{2.2}$$

with $\chi : \mathbb{R} \to [0,1]$ a Lipschitz continuous function with support contained in $[0,1]$ and $\sigma \geq 0$.

3. One has $(m_0^{(i)}, n_0^{(i)}, h_0^{(i)}, y_0^{(i)}) \in [0,1]^4$ a.s.

These assumptions cover, for parameters $a_r^x, a_d^x > 0$, functions of the form

$$\rho_x(V) = \frac{a_r^x (V - V_r^x)}{1 - \exp\left(-\lambda_r^x (V - V_r^x)\right)}, \quad \zeta_x(V) = a_d^x \exp\left(-\lambda_d^x (V - V_d^x)\right), \tag{2.3}$$

for $x = m, n$, and

$$\rho_h(V) = a_r^h \exp\left(-\lambda_r^h (V - V_r^h)\right), \quad \zeta_h(V) = \frac{a_d^h}{1 + \exp\left(-\lambda_d^h (V - V_d^h)\right)}, \tag{2.4}$$

considered in the original HH model [26], as well as functions

$$\rho_y(V) = \frac{a_r^y T_{\max}}{1 + \exp\left(-\lambda (V - V_T)\right)}, \quad \zeta_y(V) = a_d^y \tag{2.5}$$

associated with synaptic channels in [14, Chapter 7]. Diffusion coefficients σ_x defined in terms of the functions ρ_x and ζ_x as in (2.2) have been considered in [8], and arise naturally in diffusive scaling limits of the hybrid models studied in [39].

Observe that for functions ρ_h, ζ_m and ζ_n as above, the coefficients of system (2.1) do not satisfy classic conditions ensuring that it is well-posed. This well-posedness will be proved in Lemma **??** below, relying on results in [8] that ensure that under Hypothesis 2.1 the processes $(m_t^{(i)}, n_t^{(i)}, h_t^{(i)}, y_t^{(i)})$ remain in $[0,1]^4$. Notice that the absolute value in (2.2) can then be removed.

Synchronization

Our results on synchronization phenomena require the following additional assumption:

Hypothesis 2.2. *Hypothesis 2.1 holds and moreover:*

4. *The parameter g_L in (1.2) (termed "leak conductance") is strictly positive.*
5. *There exists a constant $V_0^{max} > 0$ not depending on N such that*

$$\sup_{i=1,\dots,N} |V_0^{(i)}| \leq V_0^{max} \quad a.s.$$

We also need to introduce notation for some empirical means, namely

$$\bar{V}_t^N = \frac{1}{N}\sum_{i=1}^N V_t^{(i)}, \quad \bar{X}_t = \frac{1}{N}\sum_{i=1}^N X_t^{(i)} \quad \text{and} \quad \bar{x}_t^N = \frac{1}{N}\sum_{i=1}^N x_t^{(i)} \ \text{ for } x = m, n, h, y.$$

Moreover, for each $N \geq 1$ and $t_1 \geq 0$ we let $(\widehat{X}_t^{N,t_1} : t \geq t_1) = \left((\widehat{V}_t^N, \widehat{m}_t^N, \widehat{n}_t^N, \widehat{h}_t^N, \widehat{y}_t^N) : t \geq t_1\right)$ denote the solution of the ordinary differential equation

$$\begin{aligned} \widehat{V}_t^N &= \widehat{V}_{t_1}^N + \int_{t_1}^t F(\widehat{V}_s^N, \widehat{m}_s^N, \widehat{n}_s^N, \widehat{h}_s^N) - J_{\text{Ch}} \widehat{y}_s^N (\widehat{V}_s^N - V_{\text{rev}}) ds, \\ \widehat{x}_t^N &= \widehat{x}_{t_1}^N + \int_{t_1}^t \rho_x(\widehat{V}_s^N)(1 - \widehat{x}_s^N) - \zeta_x(\widehat{V}_s^N)\widehat{x}_s^N ds, \quad x = m, n, h, y. \end{aligned} \tag{2.6}$$

with random initial condition

$$\widehat{X}_{t_1}^{N,t_1} = \bar{X}_{t_1}^N.$$

We are now is position to state our main result about synchronization of the system (2.1):

Theorem 2.3. *Assume Hypothesis 2.2 holds and that $(X_0^{(1)}, \dots, X_0^{(N)})$ is an exchangeable random vector.*

a) **Synchronization.** *There exist constants $J_E^0 > 0$, $C_{\zeta,\rho}^0 > 0$ and $\lambda^0 > 0$ not depending on $N \geq 1$, $\sigma \geq 0$ or X_0, and there exists a time $t_0 \geq 0$ not depending on $N \geq 1$ or $\sigma \geq 0$, such that for each $J_E > J_E^0$ the solution X of (2.1) satisfies, for every $t \geq t_0$ and each $i \in \{1, \dots, N\}$:*

$$\mathbb{E}\left(|X_t^{(i)} - \bar{X}_t|^2\right) \leq \mathbb{E}\left(|X_{t_0}^{(i)} - \bar{X}_{t_0}|^2\right) e^{-\lambda^0 (t - t_0)} + \sigma^2 \frac{C_{\zeta,\rho}^0}{\lambda^0}. \tag{2.7}$$

In particular, $\limsup_{t\to\infty} \mathbb{E}\left(|X_t^{(i)} - \bar{X}_t|^2\right) \leq \sigma^2 \frac{C_{\zeta,\rho}^0}{\lambda^0}$.

b) **Synchronized dynamics.** *Assume $J_E > J_E^0$. Then, there are constant $K_0, K_0' > 0$ depending only on the parameters of the voltage dynamics in (1.2) and, for each $\delta \geq 0$, constants $K_\delta, K_\delta' > 0$ depending on the coefficients in (2.1) and on δ (increasingly) but not on N, such that for every $t_1 \geq t_0$ and each $i \in \{1, \dots, N\}$:*

$$\sup_{t_1 \leq t \leq t_1+\delta} \mathbb{E}\left(|X_t^{(i)} - \widehat{X}_t^{t_1,N}|^2\right) \leq K_0 \wedge 2\left[\left(K_0' e^{-\lambda_0(t_1-t_0)} + \sigma^2 \frac{C^0_{\zeta,\rho}}{\lambda^0}\right)(1+\delta K_\delta) + \delta K_\delta' \frac{\sigma^2}{N} C^0_{\zeta,\rho}\right]. \tag{2.8}$$

Some remarks on this result are in order:

Remark 2.4.

(i) The constants $C^0_{\zeta,\rho}$ and t_0 depend explicitly on the coefficients of the systems, with the latter possibly depending also on V_0^{max}. On the other hand, bounds for λ_0 and J_E^0 which do not depend on the initial data can also be obtained. The remaining constants are explicit and do not depend on the initial condition. No constant is claimed to be optimal.

(ii) The bound K_0 in Theorem 2.3 b) is deduced from global bounds (which we establish) on the voltage processes and their average, and its role is only to prevent the r.h.s. from growing arbitrarily with δ. The estimate becomes informative as $t_1 \to \infty$ for small enough $\sigma^2 > 0$, $\delta > 0$ and N^{-1}, and for any $\delta > 0$ and N if $\sigma^2 = 0$.

(iii) Aside from the assumption that $g_L > 0$, Theorem 2.3 holds whatever are the values of the parameters of voltage dynamics F in (1.2), and in particular if the input current I is replaced by a uniformly bounded function or (suitably measurable) process.

(iv) The exchangeability assumption can be removed at the price of adding inside the expectations in (2.7) and (2.8) the averages over i.

Mean field limit

We next address the question of the behavior of system (2.1) as $N \to \infty$. We need to introduce additional notation:

- We denote by $\mathcal{P}(\mathbb{R} \times [0,1]^4)$ the space of Borel probability measures on $\mathbb{R} \times [0,1]^4$ endowed with the weak topology, and by $\mathcal{P}_2(\mathbb{R} \times [0,1]^4)$ its subspace of probability measures with finite second moment, endowed with the Wasserstein distance $\mathcal{W}_2$. That is, for all $\mu_1, \mu_2 \in \mathcal{P}_2(\mathbb{R} \times [0,1]^4)$,

$$\mathcal{W}^2(\mu_1, \mu_2) = \inf_{\mu \in \Pi(\mu_1,\mu_2)} \int_{\mathbb{R}^5} |r_1 - r_2|^2 \mu(dr_1, dr_2),$$

  with $\Pi(\mu_1, \mu_2)$ the set of probability measures on $(\mathbb{R} \times [0,1]^4)^2$ with first and second marginals equal to μ_1 and μ_2 respectively. It is well known that the infimum is attained and that $\mathcal{W}_2$ defines a complete metric on $\mathcal{P}_2(\mathbb{R} \times [0,1]^4)$ inducing the weak topology, strengthened with the convergence of second moments (see Villani [43] for the relevant properties of Wasserstein metrics).

- Elements of $\mathbb{R} \times [0,1]^4$ describing the state space of a single neuron's dynamics will be written in the form $(v, u) = (v, (u_m, u_n, u_h, u_y))$, with $u = (u_m, u_n, u_h, u_y) \in [0,1]^4$.

- We introduce the function $\Phi : (\mathbb{R} \times [0,1]) \times (\mathbb{R} \times [0,1]^4) \to \mathbb{R}$ given by

$$\Phi(w, z, v, u) = F(v, u_m, u_n, u_h) - J_{\mathrm{E}}(v - w) - J_{\mathrm{Ch}} z (v - V_{\mathrm{rev}})$$

  and, for each channel type $x = m, n, h, y$, we define functions $b_x, a_x : \mathbb{R} \times [0,1]^4 \to \mathbb{R}$ by

$$\begin{aligned} b_x(v,u) :=& \rho_x(v)(1-u_x) - \zeta_x(v) u_x \quad \text{and} \\ a_x(v,u) :=& (\rho_x(v)(1-u_x) + \zeta_x(v) u_x)\chi(u_x) \end{aligned}$$

  (that is, $\sigma_x^2(v, u_x) = \sigma^2 a_x(v, u)$).

- Given $\mu \in \mathcal{P}_2(\mathbb{R}\times[0,1]^4)$ we write

$$\begin{aligned}\langle \mu^V\rangle &= \int_{\mathbb{R}^5} v\mu(dv,du_m,du_n,du_h,du_y) \in \mathbb{R},\\ \langle \mu^x\rangle &= \int_{\mathbb{R}^5} u_x\mu(dv,,du_m,du_n,du_h,du_y) \in [0,1] \text{ for } x=m,n,h,y \text{ and}\\ \langle \mu\rangle &= (\langle \mu^V\rangle, (\langle \mu^x\rangle)_{x=m,n,h,y}) \in \mathbb{R}\times[0,1]^4.\end{aligned}$$

- Finally, with δ_x denoting the Dirac mass at $x \in \mathbb{R}\times[0,1]^4$, we write

$$\mu_t^N := \frac{1}{N}\sum_{i=1}^N \delta_{X_t^{(i)}} \in \mathcal{P}_2(\mathbb{R}\times[0,1]^4) \tag{2.9}$$

for the empirical measure of system (2.1) at time $t \geq 0$.

Theorem 2.5. *Assume Hypothesis 2.2 and moreover that for all $N \geq 1$, $(X_0^{(1)},\dots,X_0^{(N)})$ are i.i.d. random vectors with (compactly supported) common law $\mu_0 \in \mathcal{P}(\mathbb{R}\times[0,1]^4)$ not depending on N.*

a) For each $T>0$, the process $(\mu_t^N : t\in[0,T])$ converges in law on $C([0,T];\mathcal{P}_2(\mathbb{R}\times[0,1]^4))$, when N tends to ∞, to a deterministic and uniquely determined flow of measure $(\mu_t : t\in[0,T])$ having uniformly bounded compact support. Moreover $(\mu_t : t\geq 0)$ in $C(\mathbb{R}^+;\mathcal{P}_2(\mathbb{R}\times[0,1]^4))$ is a global solution (in the sens of distribution) of the non linear McKean-Vlasov Fokker Planck equation

$$\partial_t\mu_t = \partial_v\left(\Phi(\langle\mu_t^V\rangle,\langle\mu_t^y\rangle,\cdot,\cdot)\mu_t\right) + \sum_{x=m,n,h,y}\frac{1}{2}\sigma^2\,\partial^2_{u_xu_x}(a_x\mu_t) - \partial_{u_x}(b_x\mu_t) \tag{2.10}$$

with initial condition μ_0.

b) There is a constant $C(T)>0$ depending on V_0^{max}, $T>0$ and on the coefficients of system (2.1), but not on N, such that

$$\sup_{t\in[0,T]}\mathbb{E}\left(\mathcal{W}_2^2(\mu_t^N,\mu_t)\right) \leq C(T)N^{-2/5}. \tag{2.11}$$

c) If additionally functions ρ_x and ζ_x are of class $C^2(\mathbb{R})$, (or of class $C^1(\mathbb{R})$ when $\sigma=0$), $(\mu_t : t\geq 0)$ given in part a) is the unique weak solution of (2.10) with initial condition μ_0 which has supports bounded uniformly in time.

Remark 2.6.

i) We have not been able to prove uniqueness of weak (measure) solutions to (2.10) in full generality. However, the global weak solution of (2.10) given by Theorem 2.5 a) is uniquely determined.

ii) Classically (see [34], [42]), convergence in law of μ_t^N to μ_t for fixed $t\geq 0$ implies the asymptotic independence as $N\to\infty$ of any subfamily $(X_t^{(1)},\dots,X_t^{(k)})$ of fixed size $k\leq N$ of system (2.1) (the propagation of chaos property). Somewhat counterintuitively, this is not incompatible with part a) of Theorem 2.3, even when $\sigma^2=0$.

iii) Parts a) and b) of Theorem 2.5 also hold for general exchangeable μ_0-chaotic initial conditions $(X_0^{(1)},\dots,X_0^{(N)})$ (that is, such that μ_0^N converges in law to μ_0 on $\mathcal{P}_2(\mathbb{R}\times[0,1]^4)$), in which case one must add a term of the form $C\mathbb{E}\left(\mathcal{W}_2^2(\mu_0^N,\mu_0)\right)$ on the right hand side of (2.11).

iv) The first assertion in Theorem 2.5 would be standard if the coefficients in (2.1) were globally Lipschitz. Under the key Hypothesis 2.2 we will be able to reduce the proof to the Lipschitz case. Moreover, this assumption will allow us to take full advantage of the estimates for empirical measures of i.i.d. samples proved in Fournier and Guillin [18], from where the convergence rate (2.11) will stem.

Equation (2.10) can be interpreted as the dynamical description of a system of infinitely many HH neurons in mean field interaction. Thanks to Theorem 2.5 and to the uniformity in N of the results in Theorem 2.3, we can now finally transfer our synchronization results to this infinite dimensional

setting. For each $t_1 \geq 0$, define $(\widehat{X}_t^{t_1,\infty} : t \geq t_1) = \Big((\widehat{V}_t^{\infty}, \widehat{m}_t^{\infty}, \widehat{n}_t^{\infty}, \widehat{h}_t^{\infty}, \widehat{y}_t^{\infty}) : t \geq t_1\Big)$ as the solution of the ordinary differential equation

$$\begin{aligned} \widehat{V}_t^{\infty} &= \widehat{V}_{t_1}^{\infty} + \int_{t_1}^{t} F(\widehat{V}_s^{\infty}, \widehat{m}_s^{\infty}, \widehat{n}_s^{\infty}, \widehat{h}_s^{\infty}) - J_{\text{Ch}}\widehat{y}_s^{\infty}(\widehat{V}_s^{\infty} - V_{\text{rev}})ds, \\ \widehat{x}_t^{\infty} &= \widehat{x}_{t_1}^{\infty} + \int_{t_1}^{t} \rho_x(\widehat{V}_s^{\infty})(1 - \widehat{x}_s^{\infty}) - \zeta_x(\widehat{V}_s^{\infty})\widehat{x}_s^{\infty} ds, \quad x = m, n, h, y\,, \end{aligned} \tag{2.12}$$

with deterministic initial condition

$$\widehat{X}_{t_1}^{t_1,\infty} = \langle \mu_{t_1} \rangle,$$

where $(\mu_t : t \geq 0) \in C([0,\infty), \mathcal{P}_2(\mathbb{R} \times [0,1]^4))$ is the global weak solution of (2.10) with initial condition μ_0 given by Theorem 2.5 a). We have:

Corollary 2.7. *Under the assumptions of Theorem 2.5 and for the same constants as in Theorem 2.3, whenever $J_E > J_E^0$ we have:*

a) For every $t \geq t_0$,

$$\mathcal{W}_2^2(\mu_t, \delta_{\langle \mu_t \rangle}) \leq \mathcal{W}_2^2(\mu_{t_0}, \delta_{\langle \mu_{t_0} \rangle}) e^{-\lambda^0 (t - t_0)} + \sigma^2 \frac{C_{\zeta,\rho}^0}{\lambda^0}. \tag{2.13}$$

In particular, $\limsup_{t\to\infty} \mathcal{W}_2^2(\mu_t, \delta_{\langle \mu_t \rangle}) \leq \sigma^2 \frac{C_{\zeta,\rho}^0}{\lambda^0}$.

b) For every $t_1 \geq t_0$ and $\delta \geq 0$ we have:

$$\sup_{t_1 \leq t \leq t_1 + \delta} \mathcal{W}_2^2(\mu_t, \delta_{\widehat{X}_t^{t_1,\infty}}) \leq K_0 \wedge 2\Big[\big(K_0' e^{-\lambda_0 (t_1 - t_0)} + \sigma^2 \frac{C_{\zeta,\rho}^0}{\lambda^0}\big)(1 + \delta K_\delta)\Big].$$

We next present some numerical simulations which illustrate the validity of our theoretical results (at least from a qualitative point of view) and moreover we explore the behavior of system (2.1) when several neurons subpopulations are considered and when only chemical interaction is present. Furthermore, in view of the numerical experiments, we discuss some of the limitations and possible extensions of our theoretical results.

3 Numerical Experiments

We have implemented numerical simulations of system (2.1) by means of a projective exponential Euler scheme which we next describe.

For a given time horizon $T > 0$ and a natural number M, we consider the time grid $\{t_0 = 0, t_1 = T/M, t_2 = 2T/M, \ldots, t_k = kT/M, \ldots, t_M = T\}$. As initial condition for each neuron in the system we consider independent random variables, uniformly distributed on $[-100, 100] \times [0,1]^4$. Given the value of the system at t_k, the value for $\widehat{V}_{t_{k+1}}^{(i)}$ is computed as the exact solution to the ODE

$$\begin{aligned} \widehat{V}_t^{(i)} = \widehat{V}_{t_k}^{(i)} &+ \int_{t_k}^{t} F(\widehat{V}_s^{(i)}, \widehat{m}_{t_k}^{(i)}, \widehat{n}_{t_k}^{(i)}, \widehat{h}_{t_k}^{(i)}) ds \\ &- \int_0^t \frac{1}{N}\sum_{j=1}^{N} J_{\text{E}}(\widehat{V}_s^{(i)} - \widehat{V}_{t_k}^{(j)}) - \frac{1}{N}\sum_{j=1}^{N} J_{\text{Ch}}\widehat{y}_{t_k}^{(j)}(\widehat{V}_s^{(i)} - V_{\text{rev}}) ds. \end{aligned}$$

which is indeed a linear ODE since F is linear in V. To compute $\widehat{x}_{t_{k+1}}^{(i)}$ we first solve the SDE

$$\begin{aligned} \widehat{z}_t^{(i)} = \widehat{x}_{t_k}^{(i)} &+ \int_{t_k}^{t} \rho_x(\widehat{V}_{t_k}^{(i)})(1 - \widehat{z}_s^{(i)}) - \zeta_x(\widehat{V}_{t_k}^{(i)})\widehat{z}_s^{(i)} ds \\ &+ \int_{t_k}^{t} \sigma_x(\widehat{V}_{t_k}^{(i)}, \widehat{x}_{t_k}^{(i)}) dW_s^{x,i}, \quad x = m, n, h, y, \end{aligned}$$

which corresponds to an Ornstein-Uhlenbeck process, so that $\widehat{z}^{(i)}_{t_{k+1}}$ can be exactly simulated. However, since conditionally on $\widehat{x}^{(i)}_{t_j}, j \leq k$ the law of $\widehat{z}^{(i)}_{t_{k+1}}$ is Gaussian, $\{\widehat{z}^{(i)}_{t_{k+1}} \notin [0,1]\}$ happens with positive probability, so we are led to define $\widehat{x}^{(i)}_{t_{k+1}}$ by projecting $\widehat{z}^{(i)}_{t_{k+1}}$ onto $[0,1]$, that is:

$$\widehat{x}^{(i)}_{t_{k+1}} = \begin{cases} 0, & \widehat{z}^{(i)}_{t_{k+1}} \in (-\infty, 0) \\ \widehat{z}^{(i)}_{t_{k+1}}, & \widehat{z}^{(i)}_{t_{k+1}} \in [0,1] \\ 1, & \widehat{z}^{(i)}_{t_{k+1}} \in (1, +\infty). \end{cases}$$

We have not yet proved the convergence of this scheme to (2.1), but we believe that it does converge at the same rate $1/2$ as the classical Euler scheme. Indeed, the convergence of a similar scheme is proved in the Appendix of Bossy et al. [7], and the arguments therein can in principle be adapted to our context (which is left for future work).

The specific values of the constants we have used in our simulations are given in Table 1, and the rate functions ρ_x and ζ_x are given in Table 2 and shown in Figure 1. Although our results hold irrespectively of the value of input current I, we have taken in all simulations $I = 25$, in which case a noiseless single neuron with the chosen parameters has a limiting regime of sustained oscillations, see Figure 2.

g_{Na}	120 [mS/cm^3]	g_{K}	36 [mS/cm^3]	g_{L}	0.3 [mS/cm^3]
V_{Na}	50 [mV]	V_{K}	-77 [mV]	V_{L}	-54.4 [mV]

Table 1: Values for the constants in the function for F. Taken from [14, p.23]

Channel type	$\rho_x(V)$	$\zeta_x(V)$
Sodium (Na) Activation Channels m	$\dfrac{0.1(V+40)}{1-\exp\left(-\dfrac{V+40}{10}\right)}$	$4\exp\left(-\dfrac{V+65}{18}\right)$
Sodium (Na) Deactivation Channels h	$0.07\exp\left(-\dfrac{V+65}{20}\right)$	$\dfrac{1}{1+\exp\left(-\dfrac{V+35}{10}\right)}$
Potassium (K) Activation Channels n	$\dfrac{0.01(V+55)}{1-\exp\left(-\dfrac{V+55}{10}\right)}$	$0.125\exp\left(-\dfrac{V+65}{80}\right)$

Table 2: Rate functions for the dynamics of the channels. Taken from [14, p.23]

3.1 Experiments illustrating our theoretical results

Our first numerical experiments illustrate the results of part a) in Theorem 2.3. In Figure 3 we show one trajectory of the system (2.1) under purely electrical interaction, for different sizes of the network and levels of noise. The first row shows the trajectories of a network of 10 neurons for $\sigma = 0$, $\sigma = 0.5$ and $\sigma = 1$. From the second to the fourth row, the trajectories of networks of 100, 1000 and 10000 neurons, respectively, are shown. The scale of all plots is the same. We observe that the qualitative behavior in terms of σ is the same for all rows: as expected, the noiseless network ultimately reaches perfect synchronization, whereas for $\sigma > 0$ the trajectories of the neurons lie in a band whose width increases with σ, as predicted by Theorem 2.3, a). Moreover, the speed at which synchronizations takes place does not depend on the size of the network nor on the level of noise.

In our second experiment, we estimate the expected value of the empirical variance of a network of various sizes and for different levels of noise. More precisely we estimate the mean of

$$\bar{S}^V_t = \frac{1}{N}\sum_{i=1}^{N}\left(V^{(i)}_t - \bar{V}^N_t\right)^2, \quad \bar{S}^x_t = \frac{1}{N}\sum_{i=1}^{N}\left(x^{(i)}_t - \bar{x}^N_t\right)^2, \quad x = m, n, h.$$

over 50000 Monte Carlo replica for each value of $\sigma \in \{0.1, 0.5, 1\}$ and $N \in \{10, 100, 1000, 10000\}$ (we now use $\sigma = 0.1$ instead of $\sigma = 0$ since in the latter case the obtained plot quickly becomes flat).

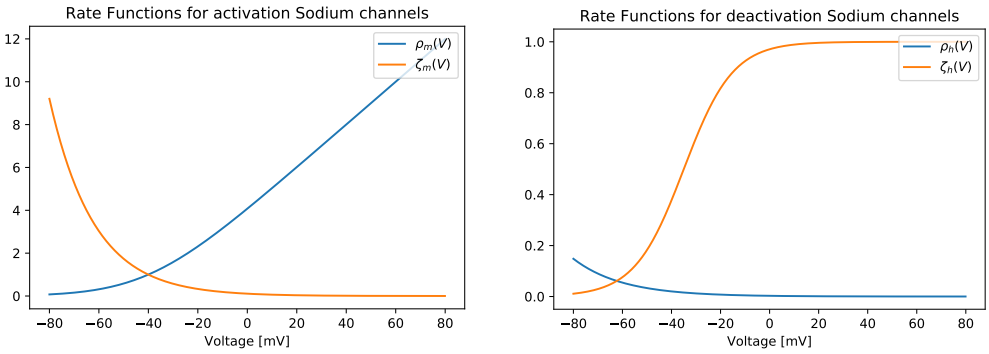

(a) Activation Sodium Channels.

(b) Deactivation Sodium Channels.

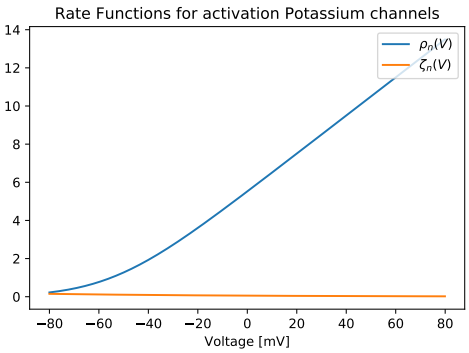

(c) Activation Potassium Channels.

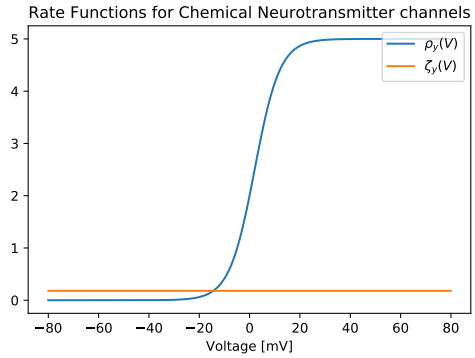

(d) Synaptic Channels.

Figure 1: Charateristic plot of rate functions ρ_x and ζ_x.

The computation of the empirical variance for each time step and replica was done using the corrected two-phase algorithm to avoid *catastrophic cancellations* (see [11]). The results of this experiment appear in Figure 4, where a different variable is presented in each row, from top to bottom: voltage (V), Sodium activation channels (m), Potassium channels (n) and Sodium deactivation channels (h). Each column corresponds to a different level of noise, increasing from $\sigma = 0.1$ on the left, to $\sigma = 0.5$ in the middle and to $\sigma = 1$ on the right. In each subfigure we show the dissipation of the expected value of the empirical variance for networks of 10, 100, 1000 and 10000 neurons. Just as for one trajectory of the system, we observe again a quick synchronization, now measured in terms of the average dispersion over many trajectories, at speed which does not depend on the noise or the size of the network, with the heights of the peaks increasing with σ. Notice that double peaks are expected from Figure 4 already: even a small dispersion of the phase among different neurons can induce a high dispersion of their voltages and channels right before and after a potential spike is emitted. This dispersion increases with N, but tends to stabilize as N becomes large (notice that the red and green lines in Figure 4 are indistinguishable), consistently with Theorem 2.5.

From this last observation, it is also interesting to point out that the maximum variance over time-windows of fixed length $\delta > 0$ which drift to infinity cannot decrease for every possible value of δ, unless $\sigma^2 = 0$. Indeed, in the noisy case the voltage of significantly many neurons can in principle differ from the voltage of the underlying one-neuron dynamics, over time-windows larger than its period, by as much as the whole asymptotic range of the voltages dynamics. Thus, albeit not sharp, the estimates in part b) of Theorem 2.3 and Corollary 2.7 are qualitatively correct.

We end the discussion on our first series of numerical experiments pointing out that, from a quantitative point of view, our theoretical results should still allow for considerable improvements. Indeed, our simulations indicate that the actual global bounds on the voltage, the critical interaction strength above which synchronization happens and the asymptotic discrepancy from synchronization are much smaller than suggested from rough estimates of the bounds in our theoretical results their proofs. In turn, the actual exponencial synchronization rate seems to be much higher. Also, our theoretical results treat the values of the voltage and channels variables jointly, although they are of considerably different orders of magnitude (i.e. channel variables and variances are negligible com-

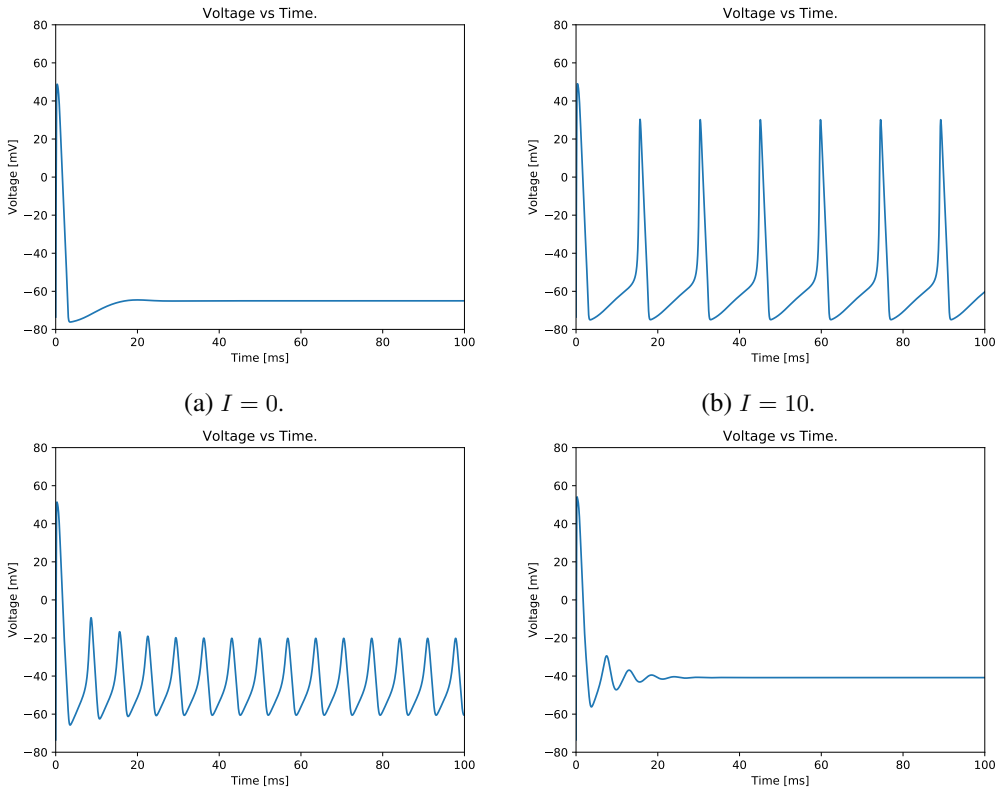

(a) $I = 0$.

(b) $I = 10$.

(c) $I = 100$.

(d) $I = 200$.

Figure 2: Reponses of the model (1.1) depending on the input current I: no oscillations if $I = 0$ (a); large amplitud and low frequency oscillations if $I = 10$ (b); small amplitud and high frequency oscillations if $I = 100$ (c); damped oscillations if $I = 200$ (d).

pared to the voltages ones). The numerical experiments show in turn that the theoretically described behavior happens at each variable's scale.

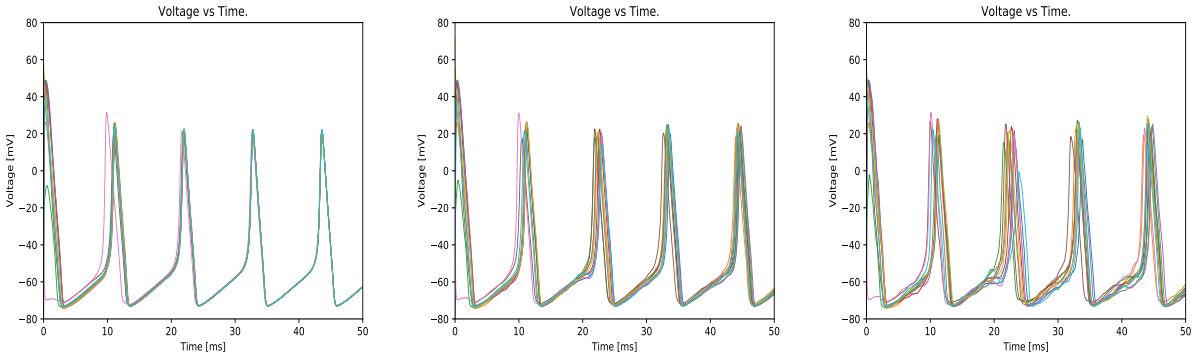

(a) $N = 10, \sigma = 0$. (b) $N = 10, \sigma = 0.5$. (c) $N = 10, \sigma = 1$.

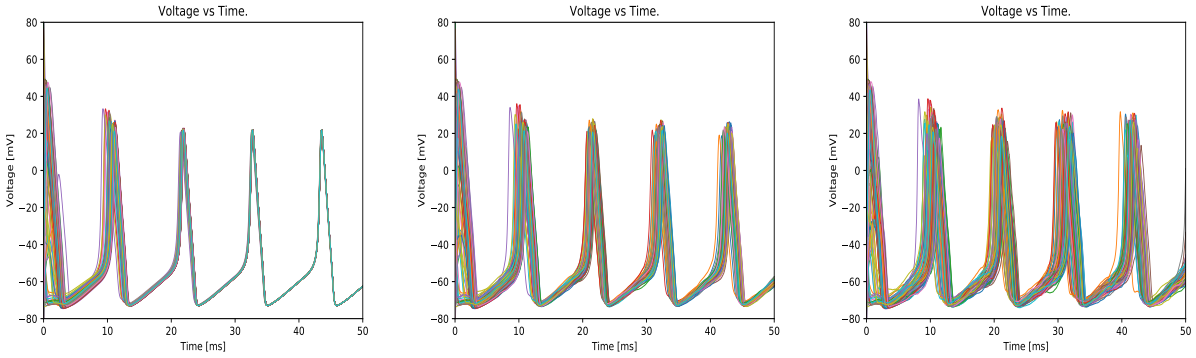

(d) $N = 100, \sigma = 0$. (e) $N = 100, \sigma = 0.5$. (f) $N = 100, \sigma = 1$.

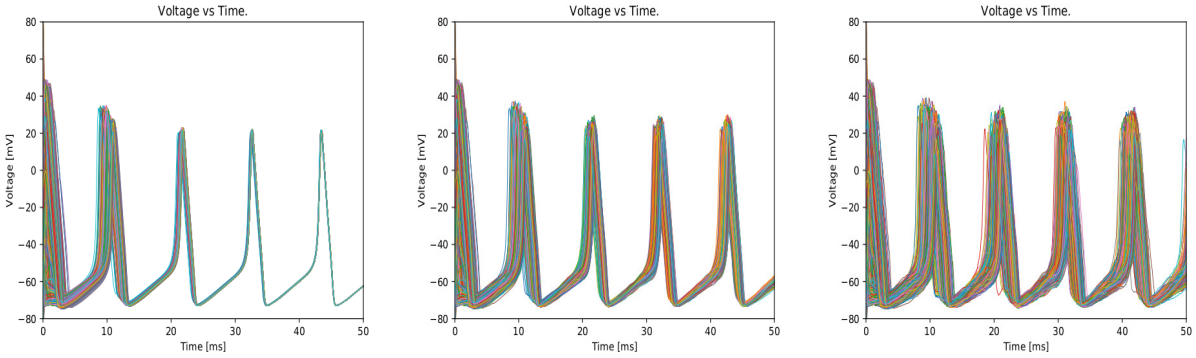

(g) $N = 1000, \sigma = 0$. (h) $N = 1000, \sigma = 0.5$. (i) $N = 1000, \sigma = 1$.

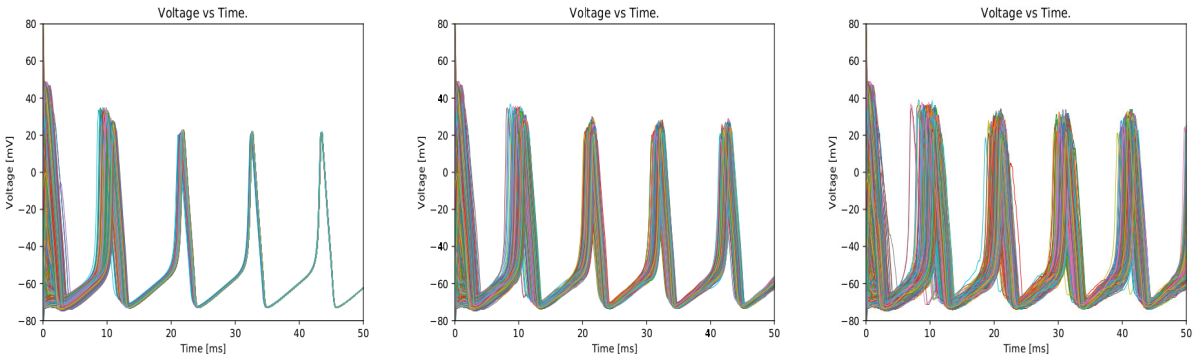

(j) $N = 10000, \sigma = 0$. (k) $N = 10000, \sigma = 0.5$. (l) $N = 10000, \sigma = 1$.

Figure 3: Synchronization of a network under pure electrical interaction for different network sizes N and noise levels σ.

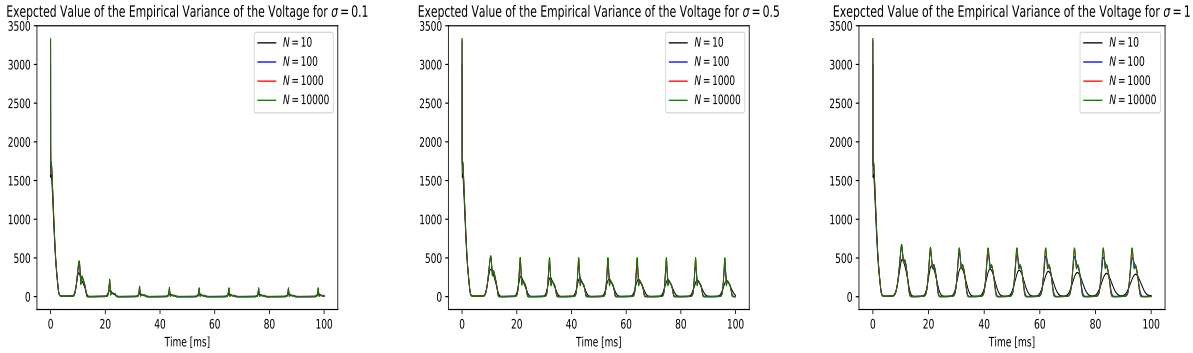

(a) V, $\sigma = 0.1$. (b) V, $\sigma = 0.5$. (c) V, $\sigma = 1$.

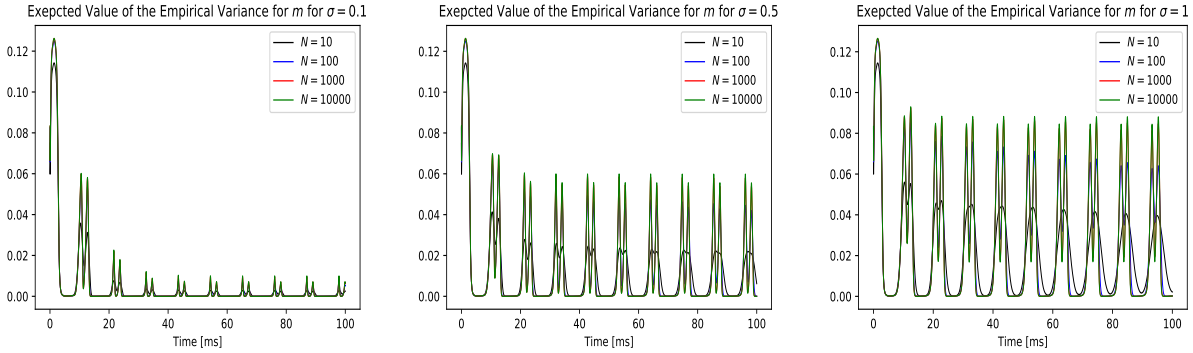

(d) m, $\sigma = 0.1$. (e) m, $\sigma = 0.5$. (f) m, $\sigma = 1$.

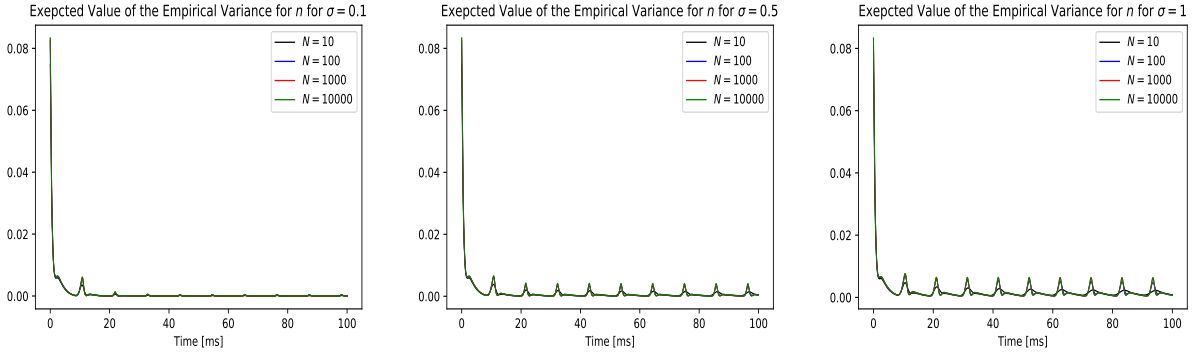

(g) n, $\sigma = 0.1$. (h) n, $\sigma = 0.5$. (i) n, $\sigma = 1$.

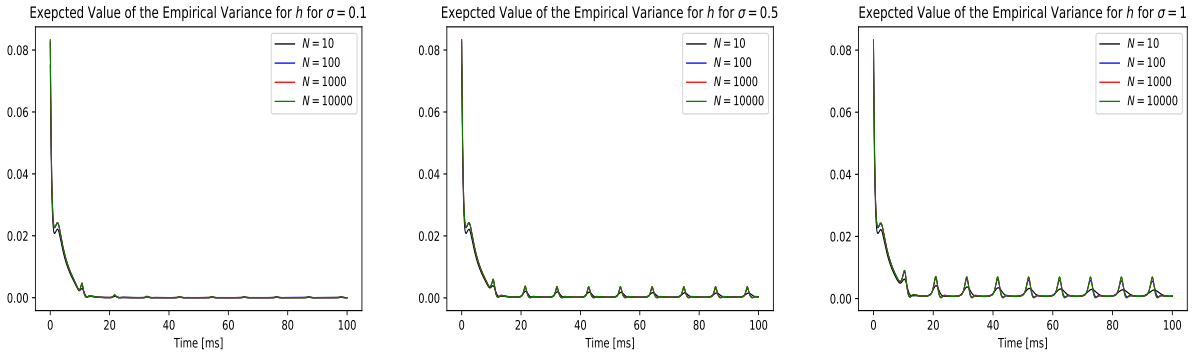

(j) h, $\sigma = 0.1$. (k) h, $\sigma = 0.5$. (l) h, $\sigma = 1$.

Figure 4: Dissipation of the empirical variance for different level of noise. First row: expected empirical variance of the voltage; second to fourth rows: expected empirical variance of the Sodium activation channels (m), the Potassium channels (n) and the Sodium deactivation channels (h) respectively. $J_{\text{Ch}} = 0$ and $J_{\text{E}} = 1$ in all simulations.

3.2 Beyond Theorem 2.3

We next carry out two type of experiments in situations not covered by our theoretical results on synchronization. In the first one we study the behavior of a more realistic network with several subpopulations of neurons. The dynamics of the i-th neuron in the subpopulation of type $\alpha \in P$, with P denoting the set of subpopulations, is given by

$$
\begin{aligned}
V_t^{(i)} &= V_0^{(i)} + \int_0^t F_\alpha(V_s^{(i)}, m_s^{(i)}, n_s^{(i)}, h_s^{(i)})ds \\
&\quad - \int_0^t \sum_{\gamma\in P} \frac{1}{N_\gamma} \sum_{j=1}^{N_\gamma} J_{\mathrm{E}}^{\alpha\gamma}(V_s^{(i)} - V_s^{(j)}) - \sum_{\gamma\in P} \frac{1}{N_\gamma} \sum_{j=1}^{N_\gamma} J_{\mathrm{Ch}}^{\alpha\gamma} y_s^{(j)}(V_s^{(i)} - V_{\mathrm{rev}}^{\alpha\gamma})ds, \\
x_t^{(i)} &= x_0^{(i)} + \int_0^t \rho_x^\alpha(V_s^{(i)})(1 - x_s^{(i)}) - \zeta_x^\alpha(V_s^{(i)})x_s^{(i)}ds \\
&\quad + \int_0^t \sigma_x^\alpha(V_s^{(i)}, x_s^{(i)})dW_s^{x,i}, \quad x = m, n, h, y\,, \qquad t \geq 0\,,
\end{aligned}
$$

where N_γ is the number of neurons in subpopulation γ. We notice that in this case the electric and chemical conductivity parameters are $|P| \times |P|$ matrices. Propagation of chaos for such systems as $N \to \infty$ was proved in [8] (though under slightly more stringent assumptions on the coefficients). In Figure 5 we show one trajectory of a network of 100 neurons with two subpopulations, each of them with 50 neurons. On the left (plot (a)), we consider the two subpopulations with different levels of noise and different input current for each of them (different F), meanwhile the electrical conductance matrix $J_{\mathrm{E}}^{\alpha\gamma}$ is homogeneous, with all the components equal to 1. We observe that the whole network gets synchronized. We believe that Theorem 2.3 can be easily extended to this case (or, more generally, when $\inf_{\alpha,\gamma\in P} J_{\mathrm{E}}^{\alpha\gamma}$ is big enough). In the middle (plot (b)), we observe that, if in addition to considering different subpopulations, the matrix J_{E} is not homogeneous (introducing some entries smaller than the largest value 1), then synchronization can be observed in each subpopulation but not globally. More precisely, in these examples the two populations synchronize out-of-phase. Finally, on the right (plot (c)), there is no evidence of synchronized dynamics when we consider one population with same F, not equally connected with two small but different values for J_{E}. We notice that this is in line with our theoretical result that thresholds the synchronization of the dynamics for a big enough $\inf_{\alpha,\gamma\in P} J_{\mathrm{E}}^{\alpha\gamma}$, even if Theorem 2.3 gives only a sufficient condition on J_{E}.

The second type of experiment concerns chemical-only synapses, that is, $J_{\mathrm{E}} = 0$. In Figure 6 we show one trajectory of a network of 100 neurons interacting through inhibitory chemical synapses (in this case, we choose $V_{\mathrm{rev}} = -75$ according to [14, p.163]). We observe an anti-phase synchronization that persists in time (see in plot (a) the transition to the stationary regime in plot (b)), in which two clusters of simultaneously firing neurons emerge. We note that the relative sizes of the two clusters is random and might change from one simulation to another one.

On the other hand, Figure 7 shows one trajectory of a network of 100 neurons interacting through excitatory chemical synapses (with $V_{\mathrm{rev}} = 0$, see [14, p.161]). Some kind of synchronization, similar to the case of purely electrical synapses (see e.g. Figure 5(a)), emerges also here, although the shape of the oscillations is different and the frequency of the spikes is smaller.

3.3 Concluding remarks

We would like to emphasis that anti- or out-of-phase- synchronization responses are not well captured with the empirical variance criteria proposed in our Theorem 2.3. In those cases, a natural, though challenging strategy would be to extend the phase reduction approach and results developed e.g. in [25] and [24] for finite deterministic networks of HH neurons, in order to obtain rigorous synchronization results in a size independent setting and in the mean field limit. Another interesting but also challenging question would consist in looking for stationary measures of the McKean-Vlasov limit equation, and then relate them to some characteristic behavior of the system and its possible synchronization regimes, in the vein of recent works of Bertini et al. [6], Giacomin et al. [21] and Luçon and Poquet [33]. This is left for future work.

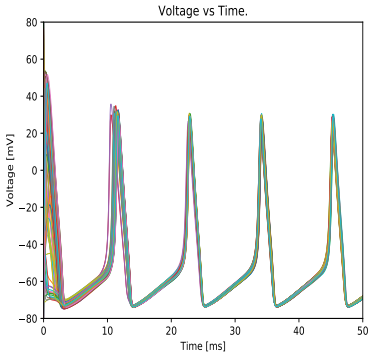

(a) Populations are different, the interaction is homogeneous.

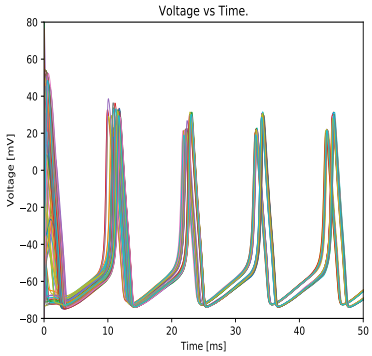

(b) Populations are different, the interaction is heterogeneous.

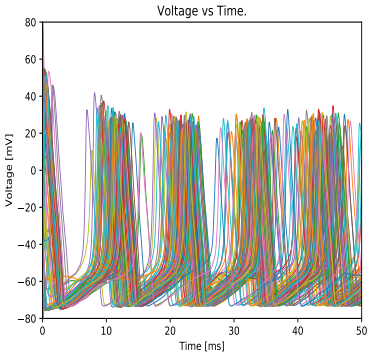

(c) Populations are equal, the interaction is heterogeneous.

Figure 5: Trajectories for network of 100 neuron with two subpopulations.

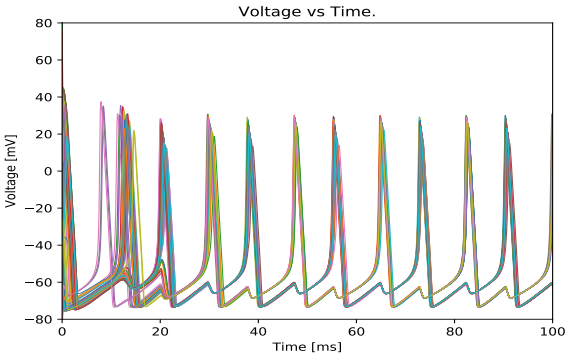

(a) Voltage of 100 neurons at the beginning of the simulation.

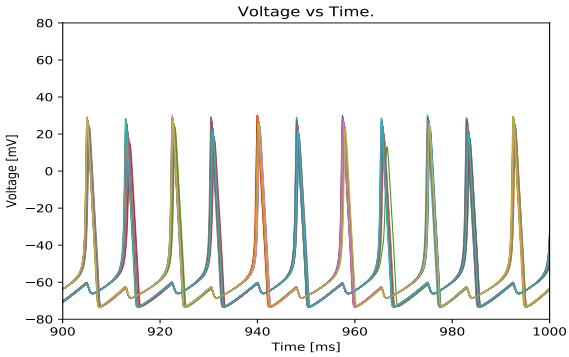

(b) Voltage of 100 neurons after 900 [ms].

Figure 6: Trajectories for network of 100 neuron with inhibitory chemical synapses

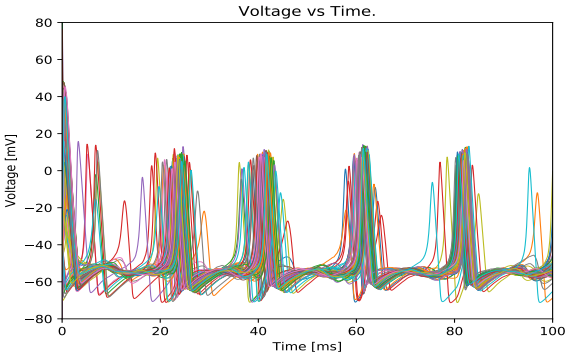

(a) Voltage of 100 neurons at the beginning of the simulation.

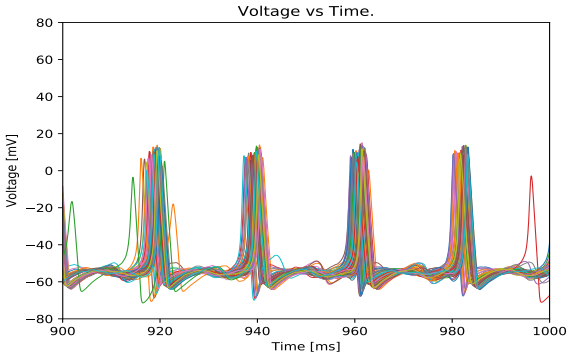

(b) Voltage of 100 neurons after 900 [ms].

Figure 7: Trajectory of a network of 100 neurons with excitatory chemical synapses

References

[1] L. Ambrosio, N. Gigli, and G. Savaré. *Gradient flows: in metric spaces and in the space of probability measures*. Springer Science & Business Media, 2008.

[2] T.D. Austin. The emergence of the deterministic hodgkin–huxley equations as a limit from the underlying stochastic ion-channel mechanism. *The Annals of Applied Probability*, 18(4):1279–1325, 2008. 2

[3] N. Axmacher, F. Mormann, G. Fernández, C. E. Elger, and J. Fell. Memory formation by neuronal synchronization. *Brain Research Reviews*, 52(1):170 – 182, 2006. 3

[4] J. Baladron, D. Fasoli, O. Faugeras, and J. Touboul. Mean field description of and propagation of chaos in networks of hodgkin-huxley and fitzhugh-nagumo neurons. *Journal of Mathematical Neuroscience*, 2(10), 2012. 3

[5] Lorenzo Bertini, Giambattista Giacomin, and Khashayar Pakdaman. Dynamical aspects of mean field plane rotators and the kuramoto model. *Journal of Statistical Physics*, 138(1):270–290, 2010. 3

[6] Lorenzo Bertini, Giambattista Giacomin, and Christophe Poquet. Synchronization and random long time dynamics for mean-field plane rotators. *Probab. Theory Related Fields*, 160(3-4):593–653, 2014. 14

[7] M. Bossy, J. Espina, J. Moricel, C. Paris, and A. Rosseau. Modeling the wind circulation around mills with a lagrangian stochastic approach. *SMAI Journal of Computational Mathematics*, 2:177–214, 2016. 9

[8] M. Bossy, O. Faugeras, and D. Talay. Clarification and complement to "mean-field description and propagation of chaos in networks of hodgkin–huxley and fitzhugh–nagumo neurons". *The Journal of Mathematical Neuroscience (JMN)*, 5(1):1–23, 2015. 2, 3, 5, 14

[9] A. N. Burkitt. A review of the integrate-and-fire neuron model: I. homogeneous synaptic input. *Biological Cybernetics*, 95(1):1–19, Jul 2006. 2

[10] A. N. Burkitt. A review of the integrate-and-fire neuron model: Ii. inhomogeneous synaptic input and network properties. *Biological Cybernetics*, 95(2):97–112, Aug 2006. 2

[11] T. Chan, G. Golub, and R. LeVeque. Algorithms for computing the sample variance: Analysis and recommendations. *The American Statistician*, 37(3):242–247, 1983. 10

[12] Ciara E. Dangerfield, David Kay, and Kevin Burrage. Modeling ion channel dynamics through reflected stochastic differential equations. *Phys. Rev. E*, 85:051907, May 2012. 2

[13] F. Delarue, J. Inglis, S. Rubenthaler, and E. Tanré. Global solvability of a networked integrate-and-fire model of mckean–vlasov type. *The Annals of Applied Probability*, 25(4):2096–2133, 2015. 3

[14] G. B. Ermentrout and D. H. Terman. *Mathematical Foundations of Neuroscience*. Springer-Verlag New York, 2010. 2, 3, 5, 9, 14

[15] O. Faugeras, J. Touboul, and B. Cessac. A constructive mean-field analysis of multi population neural networks with random synaptic weights and stochastic inputs. *Frontiers in Computational Neuroscience*, 3:1, 2009. 3

[16] R. FitzHugh. Impulses and physiological states in theoretical models of nerve membrane. *Biophysical Journal*, 1(6):445–466, 1961. 2

[17] N. Fournier and E. Löcherbach. On a toy model of interacting neurons. *https://arxiv.org/abs/1410.3263*, 2014. 3

[18] Nicolas Fournier and Arnaud Guillin. On the rate of convergence in Wasserstein distance of the empirical measure. *Probability Theory and Related Fields*, 162(3-4):707–738, 2015. 7

[19] A. Friedman. *Stochastic differential equations and applications*. Dover Publications Inc., Mineola, NY, 2006. Two volumes bound as one, Reprint of the 1975 and 1976 original published in two volumes.

[20] J. Gärtner. On the McKean-Vlasov limit for interacting diffusions. *Mathematische Nachrichten*, 137:197–248, 1988.

[21] Giambattista Giacomin, Eric Luçon, and Christophe Poquet. Coherence stability and effect of random natural frequencies in populations of coupled oscillators. *J. Dynam. Differential Equations*, 26(2):333–367, 2014. 14

[22] Joshua H Goldwyn, Nikita S Imennov, Michael Famulare, and Eric Shea-Brown. Stochastic differential equation models for ion channel noise in hodgkin-huxley neurons. *Physical Review E*, 83(4):041908, 2011. 2

[23] Joshua H Goldwyn and Eric Shea-Brown. The what and where of adding channel noise to the hodgkin-huxley equations. *PLoS Computational Biology*, 7(11):e1002247, 2011. 2

[24] D Hansel and G Mato. Patterns of synchrony in a heterogeneous hodgkin-huxley neural network with weak coupling. *Physica A: Statistical Mechanics and its Applications*, 200(1-4):662–669, 1993. 3, 14

[25] D Hansel, G_ Mato, and C Meunier. Phase dynamics for weakly coupled hodgkin-huxley neurons. *EPL (Europhysics Letters)*, 23(5):367, 1993. 3, 14

[26] A. Hodgkin and A. Huxley. A quantitative description of membrane current and its application to conduction and excitation in nerve. *J Physiol*, 117, 1952. 1, 2, 5

[27] S. G. Hormuzdi, M. A. Filippov, G. Mitropoulou, H. Monyer, and R. Bruzzone. Electrical synapses: a dynamic signaling system that shapes the activity of neuronal networks. *Biochimica et Biophysica Acta (BBA) - Biomembranes*, 1662(1–2):113 – 137, 2004. The Connexins. 4

[28] E. M. Izhikevich. *Dynamical Systems in Neuroscience*. The MIT Press, 2007. 2, 3

[29] P. Jiruska, M. de Curtis, J. G. R. Jefferys, C. A. Schevon, S. J. Schiff, and K. Schindler. Synchronization and desynchronization in epilepsy: controversies and hypotheses. *The Journal of Physiology*, 591(4):787–797, 2013. 3

[30] I. Karatzas and S. Shreve. *Brownian Motion and Stochastic Calculus*. Graduate Texts in Mathematics. Springer, 2nd edition, 1991.

[31] Y. Kuramoto. *Chemical Oscillations, Waves, and Turbulence*. Springer Berlin Heidelberg, 1984. 3

[32] L. Lapicque. Recherches quantitatives sur l'excitation électrique des nerfs traitée comme une polarization. *J Physiol Pathol Gen (Paris)*, 9:620–635, 1907. 2

[33] E. Luçon and C. Poquet. Long time dynamics and disorder-induced traveling waves in the stochastic Kuramoto model. *Ann. Inst. Henri Poincaré Probab. Stat.*, 53(3):1196–1240, 2017. 14

[34] S. Méléard. Asymptotic behaviour of some interacting particle systems; mckean-vlasov and boltzmann models. In *Probabilistic models for nonlinear partial differential equations*, pages 42–95. Springer, 1996. 3, 7

[35] S. Mischler, C. Quiñinao, and J. Touboul. On a kinetic fitzhugh–nagumo model of neuronal network. *Communications in Mathematical Physics*, 342(3):1001–1042, 2016. 3

[36] C. Morris and H. Lecar. Voltage oscillations in the barnacle gian muscle fiber. *Biophysical Journal.*, 31(1):193–213, 1981. 2

[37] J. Nagumo, S. Arimoto, and S. Yoshizawa. An active pulse transmission line simulating nerve axon. *Proceedings of the IRE*, 1962. 2

[38] Srdjan Ostojic, Nicolas Brunel, and Vincent Hakim. Synchronization properties of networks of electrically coupled neurons in the presence of noise and heterogeneities. *Journal of Computational Neuroscience*, 26(3):369, Nov 2008. 3

[39] K. Pakdaman, M. Thieullen, and G. Wainrib. Fluid limit theorems for stochastic hybrid systems with aplication to neuron models. *Adv. in Appl. Probab.*, 42(3):761–794, 09 2010. 2, 5

[40] Benoît Perthame and Delphine Salort. On a voltage-conductance kinetic system for integrate and fire neural networks. *Kinetic and Related Models*, 6(4):841–864, 2013. 3

[41] Laura Sacerdote and Maria Teresa Giraudo. *Stochastic Integrate and Fire Models: A Review on Mathematical Methods and Their Applications*, pages 99–148. Springer Berlin Heidelberg, Berlin, Heidelberg, 2013. 2

[42] A.-S. Sznitman. Topics in propagation of chaos. In *Ecole d'été de probabilités de Saint-Flour XIX—1989*, pages 165–251. Springer, 1991. 3, 7

[43] Cédric Villani. *Optimal transport, old and new*, volume 338 of *Grundlehren der Mathematischen Wissenschaften [Fundamental Principles of Mathematical Sciences]*. Springer-Verlag, Berlin, 2009. 6

[44] G. Wainrib. *Randomness in neurons: a multiscale probabilistic analysis*. PhD thesis, École Polytechnique, 2010. 2, 3